Supplemental Information for:

# *ZmCCT* and the genetic basis of daylength adaptation underlying the post-domestication spread of maize

Hsiao-Yi Hung, Laura Shannon, Feng Tian, Peter J. Bradbury, Charles Chen, Sherry A. Flint-Garcia, Michael D. McMullen, Doreen Ware, Edward S. Buckler, John F. Doebley, and James B. Holland

## SI Materials and Methods

*Phenotypic evaluation of photoperiod response*

Anthesis date was recorded as the date on which 50% of the plants in a plot had begun shedding pollen and silking date on which 50% of the plants in a plot had visible silks. The number of days from planting to anthesis and silk dates were converted to growing degree days (1, 2). GDD to anthesis and silking were analyzed separately for long daylength and short daylength environments to obtain best linear unbiased predictions (BLUPs) of RIL values for each combination of flowering trait and daylength (3) . Photoperiod response for each RIL was computed as the difference between its GDD to flowering under long daylength and short daylength environments.

*Joint linkage QTL mapping*

Joint linkage mapping was performed by fitting family main effects and conducting stepwise model selection of SNP marker within family effects (4). Thresholds for declaring a significant marker-QTL association were obtained by permutation testing with 1000 permutations of each trait data set (5). The identified QTL positions were then optimized by iteratively testing the adjacent eight markers on both sides of each QTL position originally identified until an optimal model fit was achieved. Support intervals for a QTL were determined by moving the QTL from its peak marker position to the nearer of the closest adjacent marker or an imputed pseudomarker 1 cM away while maintaining family main effects and other QTL at their peak positions. If the QTL effect remained significant at $P \leq 0.05$ at the modified position, then the next adjacent marker or pseudomarker was tested. This process was continued in each direction away from the peak position until the marker effect was no longer significant, at which point the support interval boundary was declared. Allelic effects for each marker and family were estimated simultaneously from the final selected joint linkage QTL model and the Benjamini-Hochberg procedure (6) was used to determine the 5% false discovery rate (FDR) threshold for declaring significant allele effects. The final QTL model was also used to predict photoperiod response of the founders by their progeny RILs. Founder predictions were generated by adding twice the sum of their QTL allelic effects and the corresponding family effect to the B73 photoperiod response. The final joint linkage model was also fit to each set of individual environment RIL BLUPs to produce estimates of environment-specific allelic effects for each founder allele at each QTL. Variance components due to family, QTL, and residual effects were estimating by fitting the final joint linkage model with all effects as random. The proportion of

phenotypic variance associated with each marker was estimated by their variance component divided by the sum of all variance components in the model.

*Genome-wide association analysis*

Genome-wide association study (GWAS) was performed by projecting 26.5 M founder SNP and 1M CNV genotypes from the maize HapMap version 2 (7) on RILs. Each maize chromosome was analyzed separately for SNP associations with photoperiod response. To control for genetic variation outside of the chromosome being tested, SNPs were tested for association with residual values resulting from fitting the photoperiod response BLUPs to the final joint linkage QTL model, excluding QTL on the test chromosome (8). GWAS was then conducted using a sub-sampling strategy, in which 100 random samples (without replacement) of 80% of the RILs from each family were tested separately for GWAS (8, 9). SNPs associated with the residual phenotypes were selected using forward regression implemented in TASSEL (10) with a significance threshold of $p<10^{-6}$. The resample model inclusion probability (RMIP)(9) for each SNP was computed as the frequency with which a SNP was included in the GWAS multiple regression model among the 100 subsample analyses.

*Candidate Gene Identification in Maize Genome*

A list of candidate genes involved in Arabidopsis photoperiod pathway was curated from published literatures and public databases, such as TAIR (www.arabidopsis.org)(11) and GRAMENE (www.gramene.org)(12). In the curation effort, we also included the candidate genes identified in photoperiod pathway, related super-pathways, and the ones that interact with flowering time pathway integrators and floral meristem identity genes.

Using Arabidopsis candidates as reference, we performed a global search on maize AGPv2 filtered gene set (release 5, www.maizesequence.org), of which maize photoperiod response orthologs are determined based on sequence similarity, coverage in homology relationships, duplication consistency score and consistency of a multiple species phylogenetic framework provided by Ensembl Compara comparative genomics pipeline (13). Input for Compara ortholog determination consists of the longest translation for each gene locus, filtered for transposons and other low-confidence genes from available whole genome sequences; clustering was performed by all-versus-all BLASTP followed by the extraction of genes linked either by best reciprocal BLAST, or BLAST score ratio larger than the threshold of 0.33 (14). For each resulting cluster, we conducted multiple alignment based on protein sequences, inferred the evolutionary relationship by reconciling gene trees with the established species tree topology and determined ortholog/paralog calling based on the internal nodes annotated to distinguish speciation/duplication events of a rooted phylogeny (13, 15). Only genes in one-to-one, one-to-many and many-to-many orthologous relationships were considered.

In addition, we positioned cloned maize genes known to affect flowering time on the reference sequence by a combination of searching for loci directly in maizegdb.org (16), and by BLAST analysis at maizesequence.org. Genes with homology to rice *Ghd7* or sorghum *Ma1*/*PRR37* were identified by protein BLAST searches of the translated published sequences against the maize reference genome at maizesequence.org, using a threshold of $E < 10^{-10}$.

Enrichment of candidate genes near GWAS associations was performed by computing the proportion of SNPs associated with photoperiod response at RMIP $\geq 0.05$ within 100kb of any gene on the candidate list and comparing that to the proportion of all 27.5M HapMap SNPs and CNVs within the same intervals.

*Maize fine-mapping chromosome 10 QTL*

Three maize fine-mapping populations were created to resolve the position of the chromosome 10 QTL. One population was created by crossing a nearly-isogenic line carrying a chromosome segment including the QTL from donor parent line Ki11 in an otherwise B73 genetic background to the B73 reference parent (Figure S4). The other two populations were heterogeneous inbred families (HIFs) created by self-fertilizing NAM RILs (one from the B73 × CML228 family and one from the B73 × CML277 family) that carried residual heterozygosity around the target gene region (Figure S4). SNP markers flanking the QTL were used to screen segregating progeny for recombination events in the target interval. Selfed progeny of selected plants were screened again to identify homozygous recombinant (HR) and non-recombinant (HNR) progeny pairs from within each $F_2$-derived family. Each selected HR and HNR pair was selfed again to create homozygous progeny lines for replicated testing (Figure S5). Paired HR and HNR families were evaluated for days to flowering in one- or two-row plots with two replications in Aurora, NY in 2010 and 2011 (long daylengths). In each field, HR and HNR from the same family were planted in adjacent plots to minimize confounding field effects on the comparisons. Flowering time of individual plants in each plot was scored. Due to low germination rates and drought stress, some rows had few plants; these were excluded from the study. Only HR or HNR subclasses with at least 10 data points in each environment were included for analysis. T-tests with Bonferroni corrections for multiple testing were used to test the significance of the flowering time difference between HR and HNR. Genotyping-By-Sequencing (GBS) (17) was used to precisely determine the recombination points in recombinants. The substitution mapping procedure widely used in fine mapping (18) was used to delimit the causal QTL region.

*Teosinte population development and genotyping*

In order to compare the QTL controlling differences in anthesis date between maize and teosinte to NAM QTL, we mapped QTL in a maize-teosinte $BC_2S_3$ population that was genotyped at 19,838 markers using GBS. In the cross, W22 was the recurrent parent and the teosinte parent was *Zea mays* subsp. *parviglumis* CIMMYT accession 8759. The 866 lines comprising the cross were grown in two blocks during summer 2009 and in an additional block in summer 2010 at the West Madison Agricultural Research Center in Madison, WI. All blocks were randomized and contained 866 plots with 10 plants per plot. Flowering time, defined as the number of days between planting and when anthers were visible on at least half the plants in the plot, was recorded for all plots. Least square means for each line were used as the phenotype values for QTL mapping, carried out using a modified version of R/qtl (19) which allows the program to take into account the $BC_2S_3$ pedigree of the lines.

The large effect QTL for days to anthesis on chromosome 10 was fine-mapped using a single maize-teosinte $BC_2S_3$ family that segregated for a 50.77 Mb chromosomal segment including the QTL region introgressed from teosinte into the W22 genetic background. Using two marker loci (PZB00409.1 at AGPv2 position 84,095,979 and PZD00143.1 at AGPv2 position 109,798,193) that flanked the QTL, we isolated 74 chromosomes with cross-overs in the QTL interval. Plants possessing these recombinant chromosomes were used to produce a set of 74 homozygous recombinant chromosome nearly isogenic lines (RC-NILs). The RC-NILs were genotyped at 31 SNP and indel markers across the region (Table S7). In the summer of 2010, the RC-NILs were grown in randomized design with four blocks at the West Madison Agricultural Research Center in Madison, WI. Each block contained 76 plots with 10 plants per plot for the 74 RC-NILs plus a homozygous maize line and a second line homozygous for the teosinte across

the entire interval. Flowering time was assessed as days to anthesis and days to silk (when anthers or silks were visible on at least half the plants in the plot, respectively). Least-square means were calculated for each RC-NIL.

To assess whether late flowering alleles are prevalent in teosinte, we compared eight indepedent teosinte alleles in families derived from crosses with maize inbred W22 (Table S8). Six of these families were $BC_1S_1$ progeny lines from crosses involving teosinte inbred lines as the teosinte parents. These six families were grown during summer 2011 at the West Madison Agricultural Research Station in Madison, WI. Each of the $BC_1S_1$ families was grown in a single plot of ~1400 plants with the genotypes randomized within the plot. For each of the six families, 190 plants were genotyped for indel polymorphisms within the first exon or upstream region of *ZmCCT* and phenotyped for days to anthesis (Table S7). The additive effect of the teosinte allele at *ZmCCT* was calculated as half the difference between the homozygous teosinte and homozygous maize genotypic classes.


1. Craufurd, P. Q., Qi, A. M., Ellis, R. H., Summerfield, R. J., Roberts, E. H., & Mahalakshmi, V. (1998) Effect of temperature on time to panicle initiation and leaf appearance in sorghum *Crop Sci.* **38,** 942-947.
2. Gilmore, E. & Rogers, J. (1958) Heat units as a method of measuring maturity in corn *Agron. J.* **50,** 611-615.
3. Hung, H. Y., Browne, C., Guill, K., Coles, N., Eller, M., Garcia, A., Lepak, N., Melia-Hancock, S., Oropeza-Rosas, M., Salvo, S*., et al.* (2012) The relationship between parental genetic or phenotypic divergence and progeny variation in the maize Nested Association Mapping population *Heredity* **108,** 490-499.
4. Buckler, E. S., Holland, J. B., McMullen, M. M., Kresovich, S., Acharya, C., Bradbury, P., Brown, P., Browne, C., Eller, M., Ersoz, E*., et al.* (2009) The genetic architecture of maize flowering time *Science* **325,** 714-718.
5. Doerge, R. W. & Churchill, G. A. (1996) Permutation tests for multiple loci affecting a quantitative character. *Genetics* **142,** 285-294.
6. Benjamini, Y. & Yekutieli, D. (2005) Quantitative trait loci analysis using the false discovery rate *Genetics* **171,** 783-789.
7. Chia, J.-M., Song, C., Bradbury, P. J., Costich, D., de Leon, N., Doebley, J., Elshire, R. J., Gaut, B., Geller, L., Glaubitz, J. C*., et al.* (2012) Maize HapMap2 identifies extant variation from a genome in flux. *Nat. Genet.***,** advance online publication 3 June 2012; DOI 2010.1039/ng.2313.

8. Tian, F., Bradbury, P. J., Brown, P. J., Flint-Garcia, S., Rocheford, T. R., McMullen, M. D., Holland, J. B., & Buckler, E. S. (2011) Genome-wide association study of leaf architecture in the maize nested association mapping population *Nat. Genet.* **43,** 159-162.
9. Valdar, W., Holmes, C. C., Mott, R., & Flint, J. (2009) Mapping in Structured Populations by Resample Model Averaging *Genetics* **182,** 1263-1277.
10. Bradbury, P. J., Zhang, Z., Kroon, D. E., Casstevens, T. M., Ramdoss, Y., & Buckler, E. S. (2007) TASSEL: software for association mapping of complex traits in diverse samples *Bioinformatics* **23,** 2633-2635.
11. Lamesch, P., Berardini, T. Z., Li, D., Swarbreck, D., Wilks, C., Sasidharan, R., Muller, R., Dreher, K., Alexander, D. L., Garcia-Hernandez, M*., et al.* (201) The Arabidopsis Information Resource (TAIR): improved gene annotation and new tools *Nucleic acids research* **doi: 10.1093/nar/gkr1090**.
12. Youens-Clark, K., Buckler, E., Casstevens, T., Chen, C., DeClerck, G., Derwent, P., Dharmawardhana, P., Jaiswal, P., Kersey, P., Karthikeyan, A. S*., et al.* (2011) Gramene database in 2010: updates and extensions *Nucleic Acids Res.* **39,** D1085-D1094.
13. Vilella, A. J., Severin, J., Ureta-Vidal, A., Heng, L., Durbin, R., & Birney, E. (2009) EnsemblCompara GeneTrees: Complete, duplication-aware phylogenetic trees in vertebrates *Genome Res.* **19,** 327-335.
14. Altschul, S. F., Gish, W., Miller, W., Myers, E. W., & Lipman, D. J. (1990) Basic Local Alignment Search Tool *J. Molec. Biol.* **215,** 403-410.
15. Schnable, P. S., Ware, D., Fulton, R. S., Stein, J. C., Wei, F., Pasternak, S., Liang, C., Zhang, J., Fulton, L., Graves, T. A*., et al.* (2009) The B73 maize genome: Complexity, diversity, and dynamics *Science* **326,** 1112-1115.
16. Schaeffer, M. L., Harper, L. C., Gardiner, J. M., Andorf, C. M., Campbell, D. A., Cannon, E. K. S., Sen, T. Z., & Lawrence, C. J. (2011) MaizeGDB: curation and outreach go hand-in-hand *Database* **doi:10.1093/database/bar022**.
17. Elshire, R. J., Glaubitz, J. C., Sun, Q., Poland, J. A., Kawamoto, K., Buckler, E. S., & Mitchell, S. E. (2011) A robust, simple Genotyping-by-Sequencing (GBS) approach for high diversity species *PLoS One* **6**.
18. Paterson, A. H., DeVerna, J. W., Lanini, B., & Tanksley, S. D. (1990) Fine mapping of quantitative trait loci using selected overlapping recombinant chromosomes, in an interspecies cross of tomato. *Genetics* **124,** 735-742.
19. Broman, K., Wu, H., Sen, Ś., & Churchill, G. (2003) R/qtl: QTL mapping in experimental crosses *Bioinformatics* **19,** 889-890.

**Supplemental Datasets** (note: zip folder containing all files available at

http://www.panzea.org/lit/publication.html#2012):

Dataset S1. Photoperiod_paper_data_supplement_raw_data.xls

Dataset S2.Photoperiod_paper_data_supplement_line_BLUPs.xls

Dataset S3. NAM_Photoperiod_QTL_Peaks_SupportIntervals_cM_AGPv2.xls

Dataset S4. Silk GDD QTL effect comparisons-long vs short day vs photo response.xls

Dataset S5.QTL x founder Effect Matrix.xls

Dataset S6.Flowering time QTL comparisons teosinte-NAM.xls

Dataset S7.Silk_photoperiod_HapMap_GWAS_hit_details.xls

Dataset S8.Final candidate gene list.xls

Dataset S9.Imputed GBS scores Ghd7 region.xls

Dataset S10. Genomic DNA sequence alignments for five regions (A1 – A5) of *ZmCCT* from 27 maize inbreds and 16 teosinte inbreds, and for one region (A6) from 230 maize inbreds and 7 teosinte inbreds. Alignments are in Phylip format.

**Supplemental Figures:**

Figure S1. Mean (and standard error) of photoperiod responses for growing degree days to (A) anthesis and (B) silking for NAM founders and NAM RIL families.

Figure S2. Heat map of QTL allele effects from NAM founders at QTL for growing degree days to anthesis.

Figure S3. Regression of observed founder BLUPs for photoperiod response measured in growing degree days to (A) anthesis and (B) silk on predicted genotypic values based on joint linkage QTL models.

Figure S4. Graphical genotypes of three initial maize lines used for constructing segregating population for fine mapping chromosome 10 flowering time QTL. (A) NIL75, a Near Isogenic Line (NIL) produced by Syngenta containing introgression from founder Ki11 in the background of B73, (B) Z005E0165, a Heterogeneous Inbred Family (HIF) heterozygous at QTL target region selected from NAM RIL population B73 X CML277, (C) Z003E0129, a Heterogeneous Inbred Family (HIF) heterozygous at QTL target region, selected from NAM RIL population B73 X CML228. Red indicatess regions homozygous for B73; blue indicates regions homozygous for non-B73 parent; green indicates heterozygous regions. The introgressions at QTL target region are indicated by arrows.

Figure S5. Procedures for fine mapping chromosome 10 flowering time QTL in maize.

Figure S6. Fine mapping chromosome 10 photoperiod response QTL in NIL75 (Ki11) × B73 maize population. Graphical genotypes of identified homozygous recombinants (HR) at the target region within each recombinant family (I through IX) are shown on left. Black or white boxes next to the HR indicate the corresponding homozygous non-recombinants (HNR) identified within each recombinant family. White, black and gray boxes indicate homozygous for donor parent allele, homozygous for B73 allele, and regions where recombination occurred, respectively. The graphs on the right are the flowering time difference between HR and HNR. Red bars and ** indicate significant difference at 0.01 after Bonferroni correction. Black bars indicate no significant difference observed between HR and HNR. NA, not available. Predicted genes from the filtered gene set are shown as blue boxes above the graphical genotypes. Candidate gene *ZmCCT* is highlighted in red.

Figure S7. Fine mapping chromosome 10 photoperiod response QTL in Z005E0165 (B73 × CML277) HIF maize population. Graphical genotypes of identified homozygous recombinants (HR) at the target region within each recombinant family (I through IX) are shown on left. Black or white boxes next to the HR indicate the corresponding homozygous non-recombinants (HNR) identified within each recombinant family. White, black and gray boxes indicate homozygous for donor parent allele, homozygous for B73 allele, and regions where recombination occurred, respectively. The graphs on the right are the flowering time difference between HR and HNR. Red bars and ** indicate significant difference at 0.01 after Bonferroni correction. Black bars indicate no significant difference observed between HR and HNR. NA, not available. Predicted genes from the filtered gene set are shown as blue boxes above the graphical genotypes. Candidate gene *ZmCCT* is highlighted in red.

Figure S8. Fine mapping chromosome 10 photoperiod response QTL in Z003E0129 (B73 × CML228) HIF maize population. Graphical genotypes of identified homozygous recombinants (HR) at the target region within each recombinant family (I through IX) are shown on left. Black or white boxes next to the HR indicate the corresponding homozygous non-recombinants (HNR) identified within each recombinant family. White, black and gray boxes indicate homozygous for donor parent allele, homozygous for B73 allele, and regions where recombination occurred, respectively. The graphs on the right are the flowering time difference between HR and HNR. Red bars and ** indicate significant difference at 0.01 after Bonferroni correction. Black bars indicate no significant difference observed between HR and HNR. NA, not available. Predicted genes from the filtered gene set are shown as blue boxes above the graphical genotypes. Candidate gene *ZmCCT* is highlighted in red.

Figure S9. Protein sequence of *ZmCCT* across NAM founders. The CCT domain is indicated in red at the C-terminus. Three NAM founders, B97, CML103 and Tzi8, are not included because they failed in sequencing one part of gene.

Figure S10. Interaction between SNP1411 or SNP1520 at *ZmCCT* and MITE at *Vgt1*. At both loci, B73 allele is coded as "0", and the alternate allele is coded as "1". The least square mean of haplotype combinations at both loci were calculated after correcting for the population structure and the genetic background effect. A significant difference (P=4.3E-09) for PPGDDTA was detected between alleles of SNP1411 or SNP1520 at *ZmCCT* in lines not containing MITE at *Vgt1*, whereas no significant difference (P=0.31) was detected between alleles of SNP1411 or SNP1520 at *ZmCC*T in lines containing MITE at *Vgt1*.

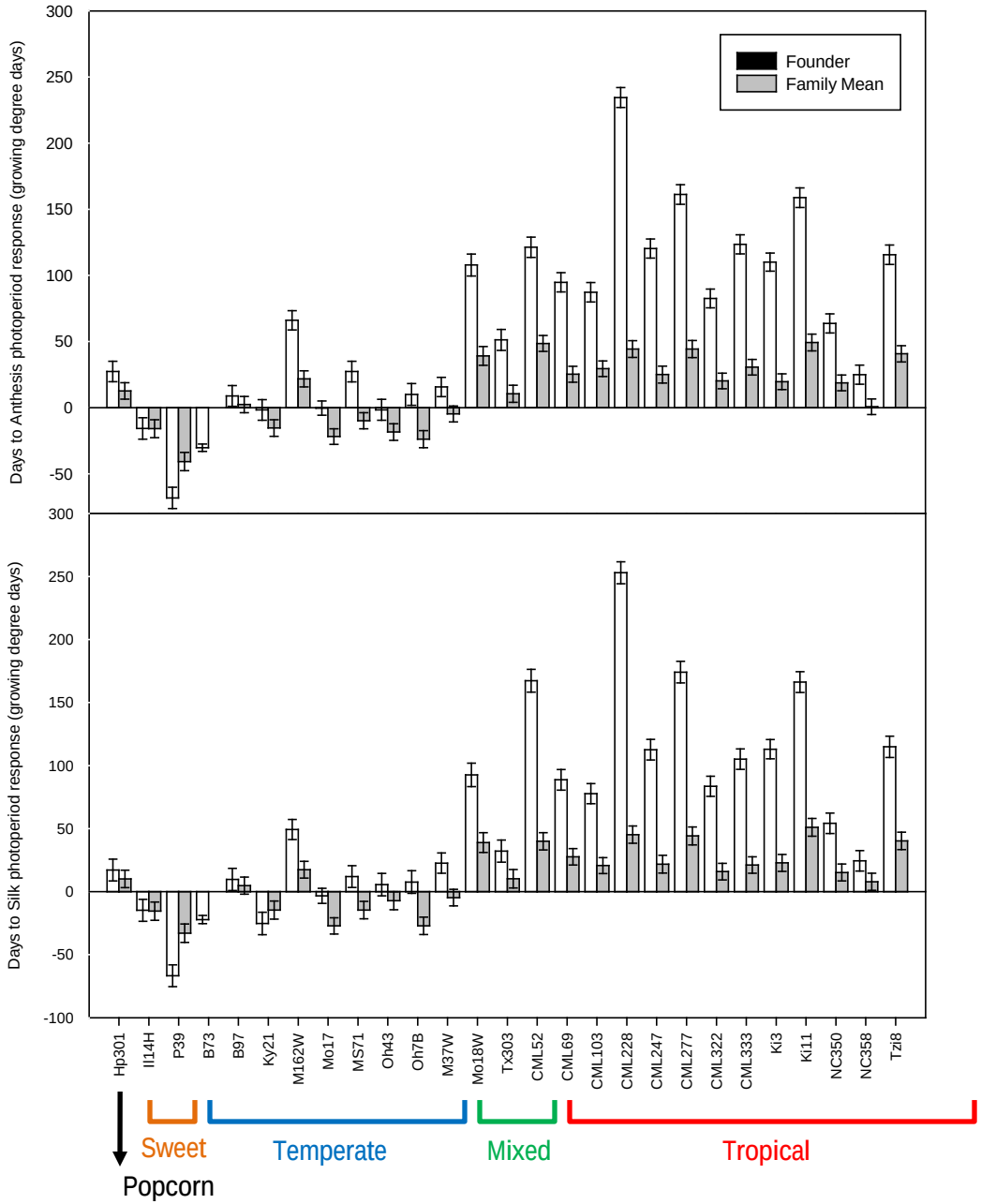
Days to Anthesis photoperiod response (growing degree days)
Days to Silk photoperiod response (growing degree days)
Founder
Family Mean
300
250
200
150
100
50
0
-50
-100
Hp301
Il14H
P39
B73
B97
Ky21
M162W
Mo17
MS71
Oh43
Oh7B
M37W
Mo18W
Tx303
CML52
CML69
CML103
CML228
CML247
CML277
CML322
CML333
Ki3
Ki11
NC350
NC358
Tzi8
Sweet
Popcorn
Temperate
Mixed
Tropical

Figure S1

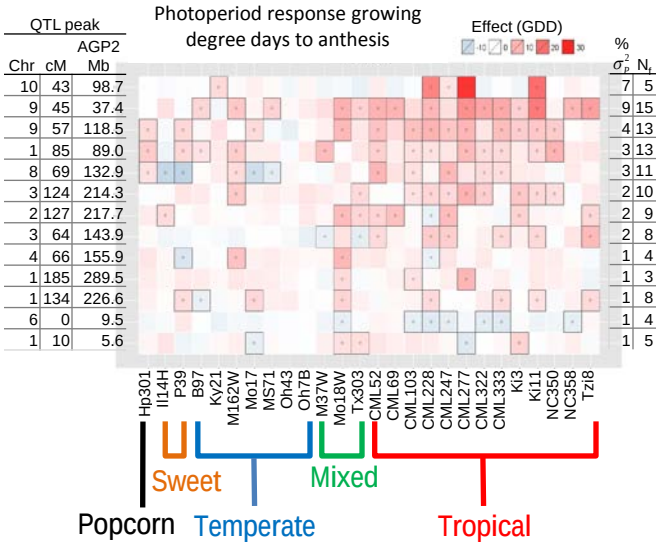
QTL peak
AGP2
Chr cM Mb
10 43 98.7
9 45 37.4
9 57 118.5
1 85 89.0
8 69 132.9
3 124 214.3
2 127 217.7
3 64 143.9
4 66 155.9
1 185 289.5
1 134 226.6
6 0 9.5
1 10 5.6
Photoperiod response growing degree days to anthesis
Effect (GDD)
% $\sigma_p^2$ $N_t$
7 5
9 15
4 13
3 13
3 11
2 10
2 9
2 8
1 4
1 3
1 8
1 4
1 5
Hp301
Il14H
P39
B97
Ky21
M162W
Mo17
MS71
Oh43
Oh7B
M37W
Mo18W
Tx303
CML52
CML69
CML103
CML228
CML247
CML277
CML322
CML333
Ki3
Ki11
NC350
NC358
Tzi8
Sweet
Mixed
Popcorn
Temperate
Tropical

Figure S2

(a)

Photoperiod response growing degree days to anthesis

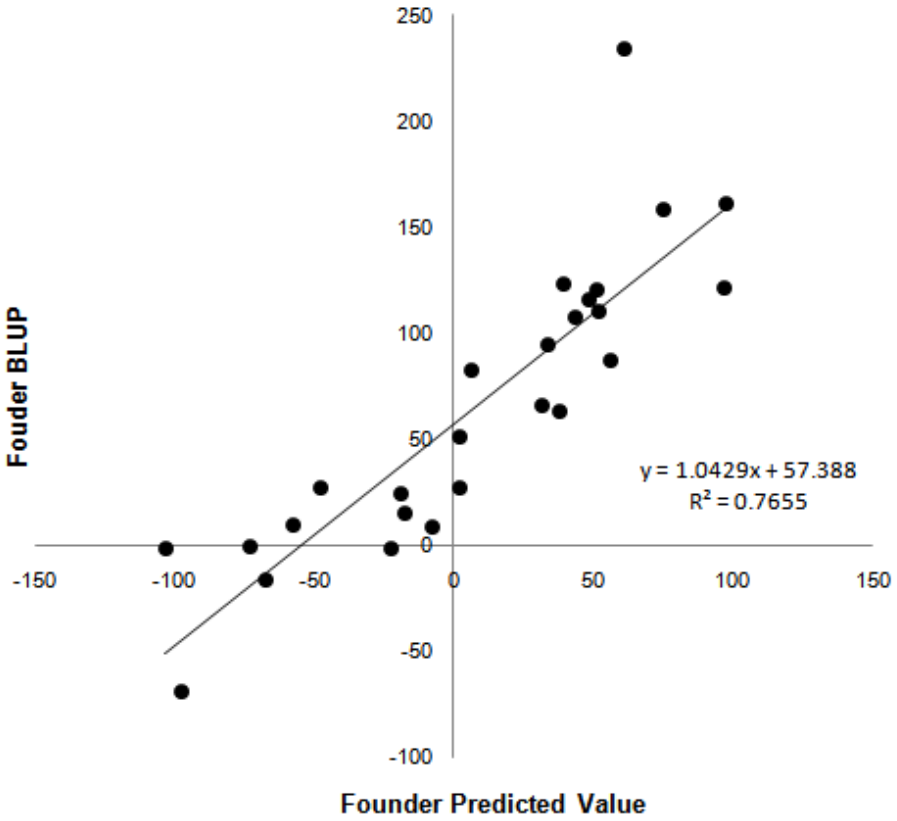


(b)

Photoperiod response growing degree days to silk

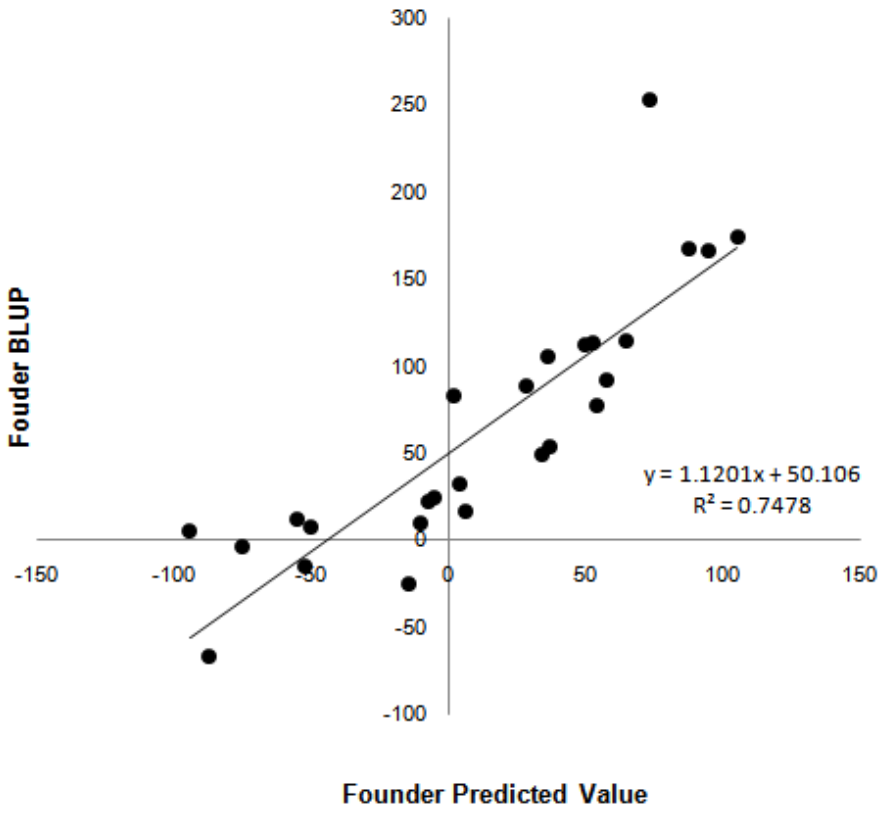


Figure S3

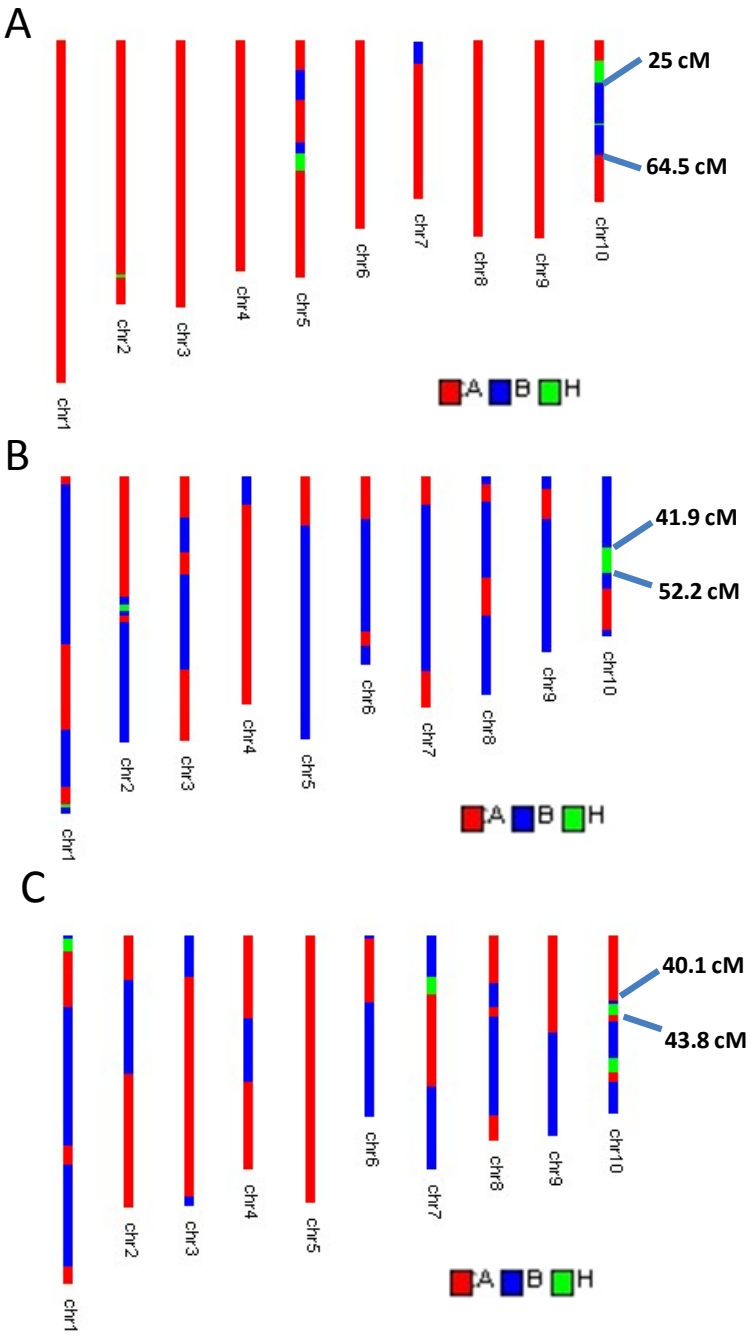
A
25 cM
64.5 cM
chr1
chr2
chr3
chr4
chr5
chr6
chr7
chr8
chr9
chr10
A B H
B
41.9 cM
52.2 cM
chr1
chr2
chr3
chr4
chr5
chr6
chr7
chr8
chr9
chr10
A B H
C
40.1 cM
43.8 cM
chr1
chr2
chr3
chr4
chr5
chr6
chr7
chr8
chr9
chr10
A B H

Figure S4

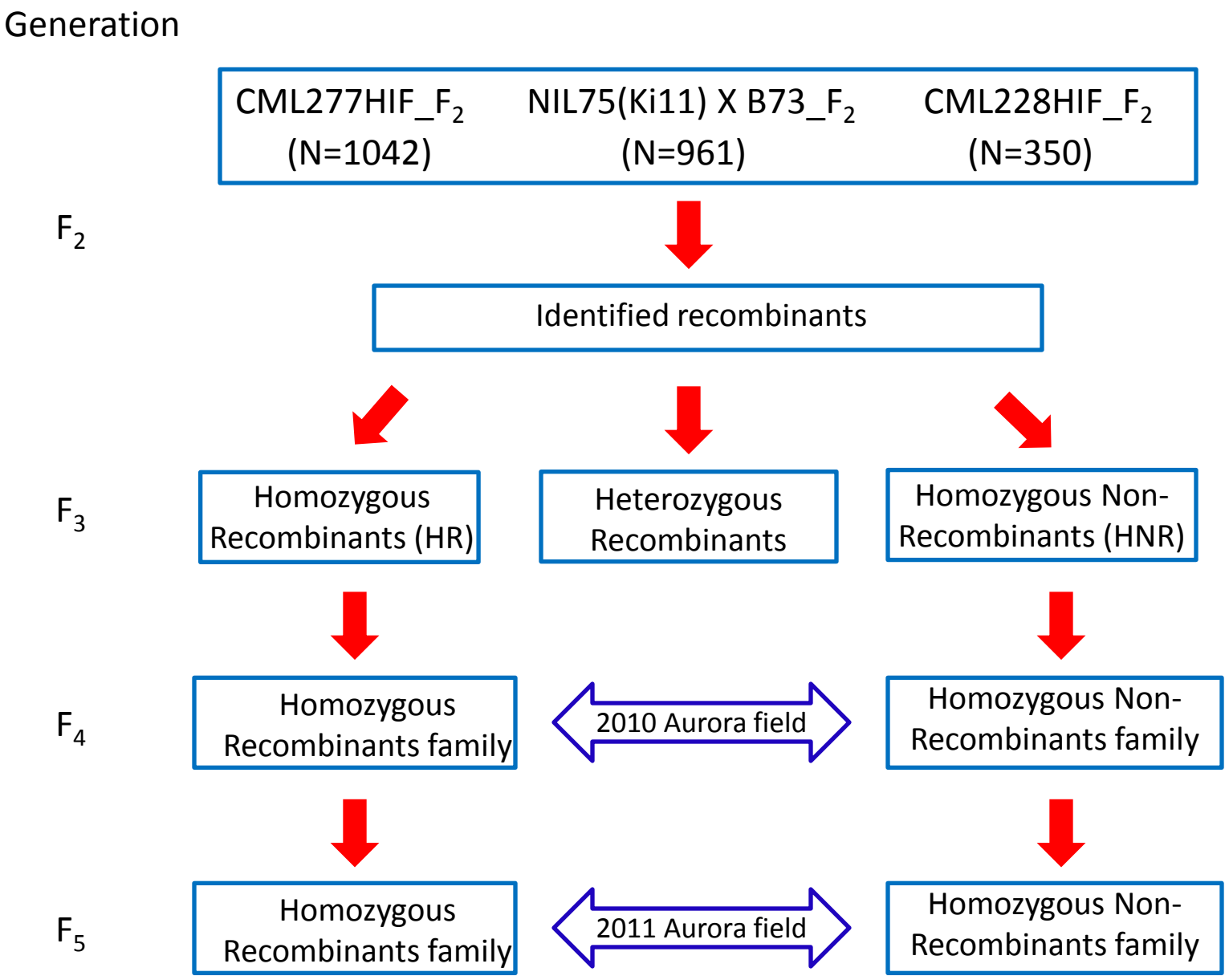
Generation
CML277HIF_F2 (N=1042)
NIL75(Ki11) X B73_F2 (N=961)
CML228HIF_F2 (N=350)
F2
Identified recombinants
F3
Homozygous Recombinants (HR)
Heterozygous Recombinants
Homozygous Non-Recombinants (HNR)
F4
Homozygous Recombinants family
2010 Aurora field
Homozygous Non-Recombinants family
F5
Homozygous Recombinants family
2011 Aurora field
Homozygous Non-Recombinants family

Figure S5

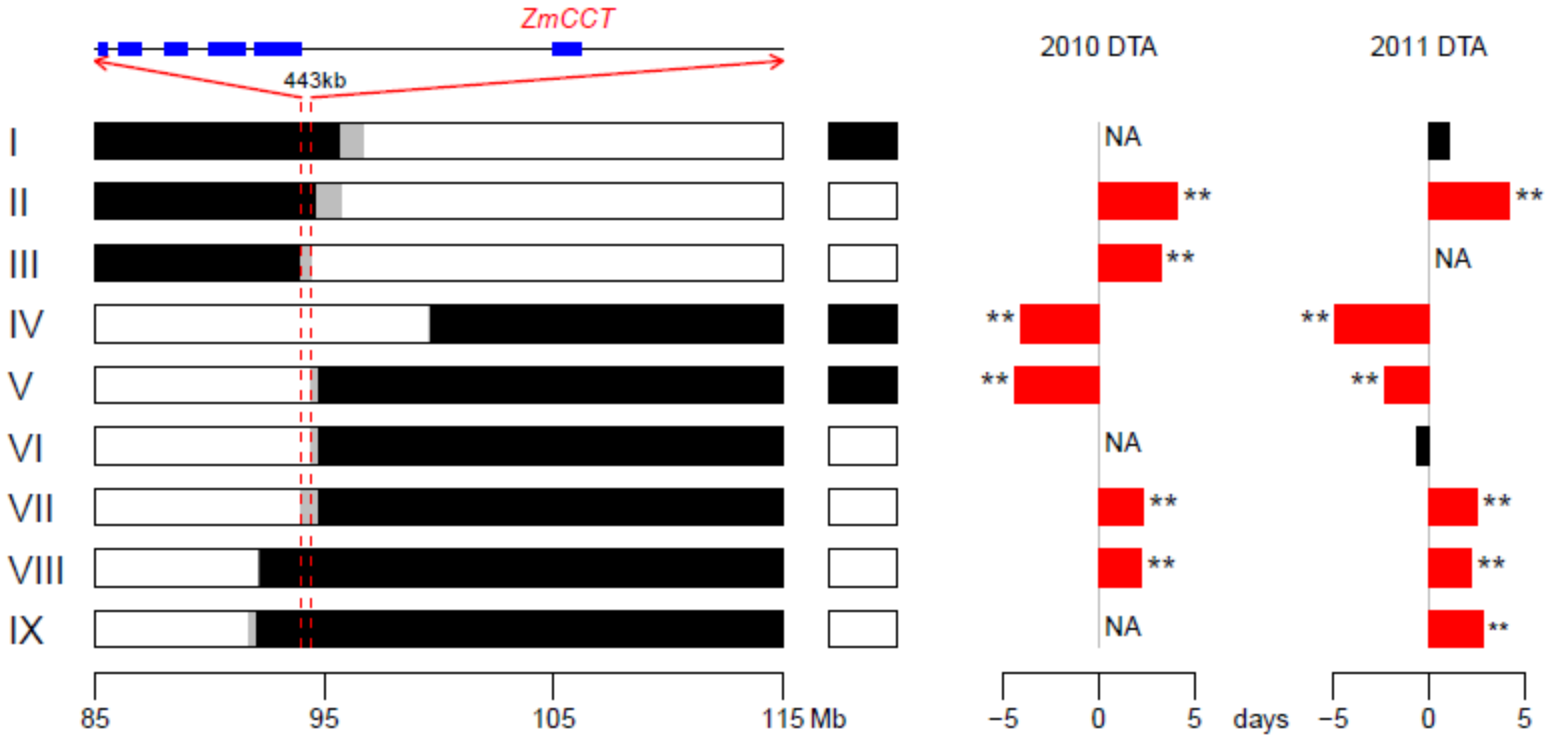
ZmCCT
443kb
I
II
III
IV
V
VI
VII
VIII
IX
85
95
105
115 Mb
2010 DTA
2011 DTA
NA
**
−5
0
5
days

Figure S6

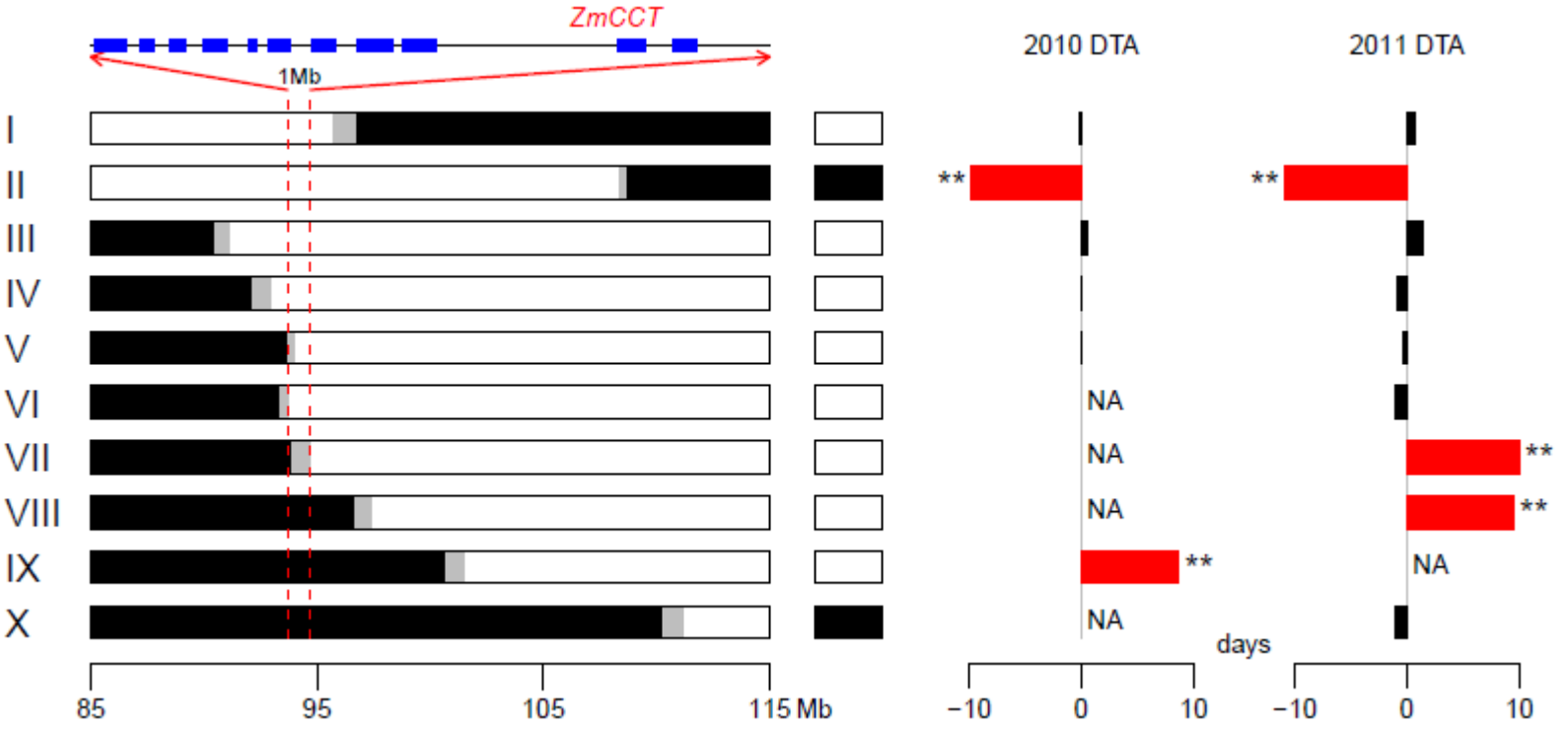
ZmCCT
1Mb
I
II
III
IV
V
VI
VII
VIII
IX
X
85
95
105
115 Mb
2010 DTA
2011 DTA
**
**
NA
NA
NA
**
NA
**
**
NA
days
−10
0
10
−10
0
10

Figure S7

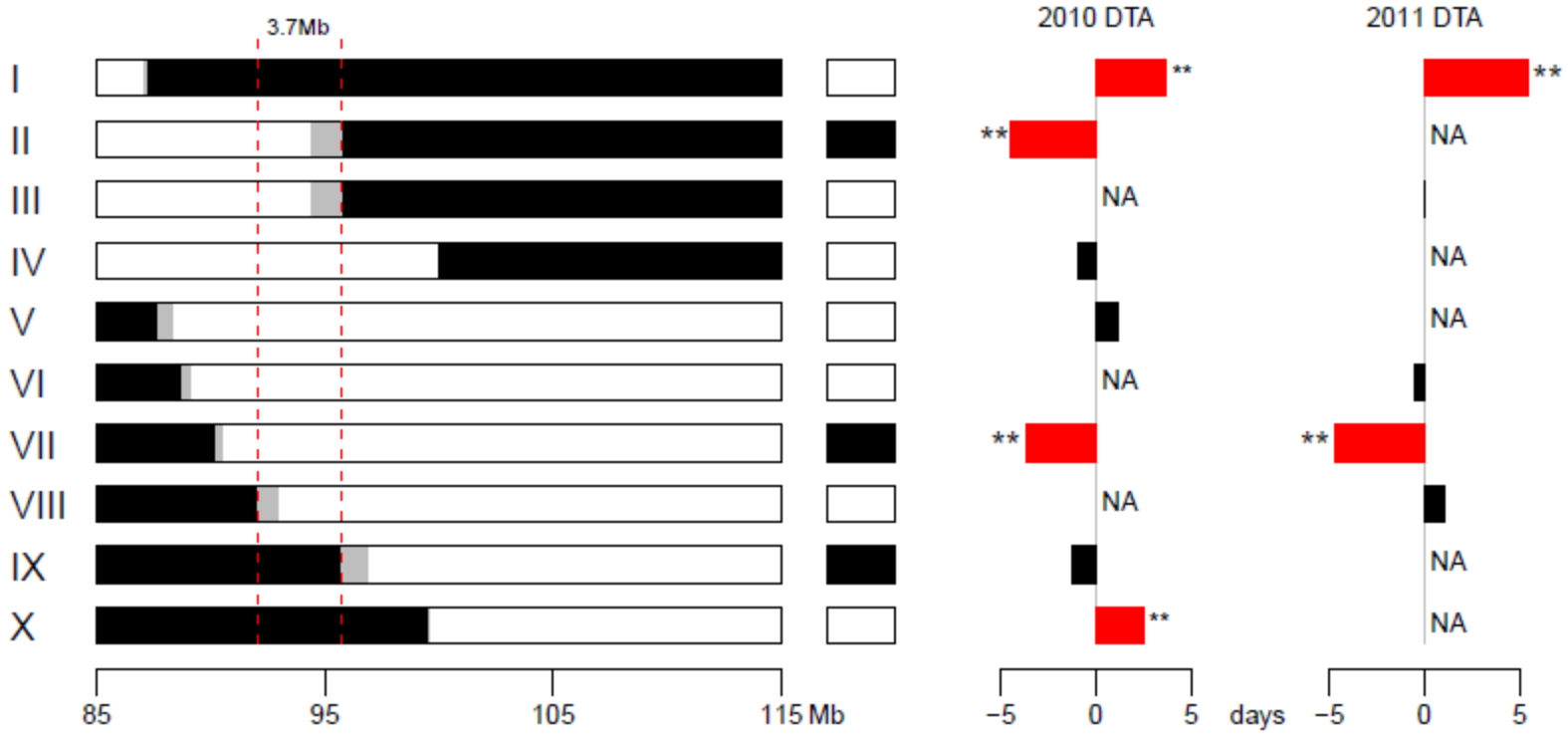
3.7Mb
I
II
III
IV
V
VI
VII
VIII
IX
X
85
95
105
115 Mb
2010 DTA
2011 DTA
**
NA
−5
0
5
days

Figure S8

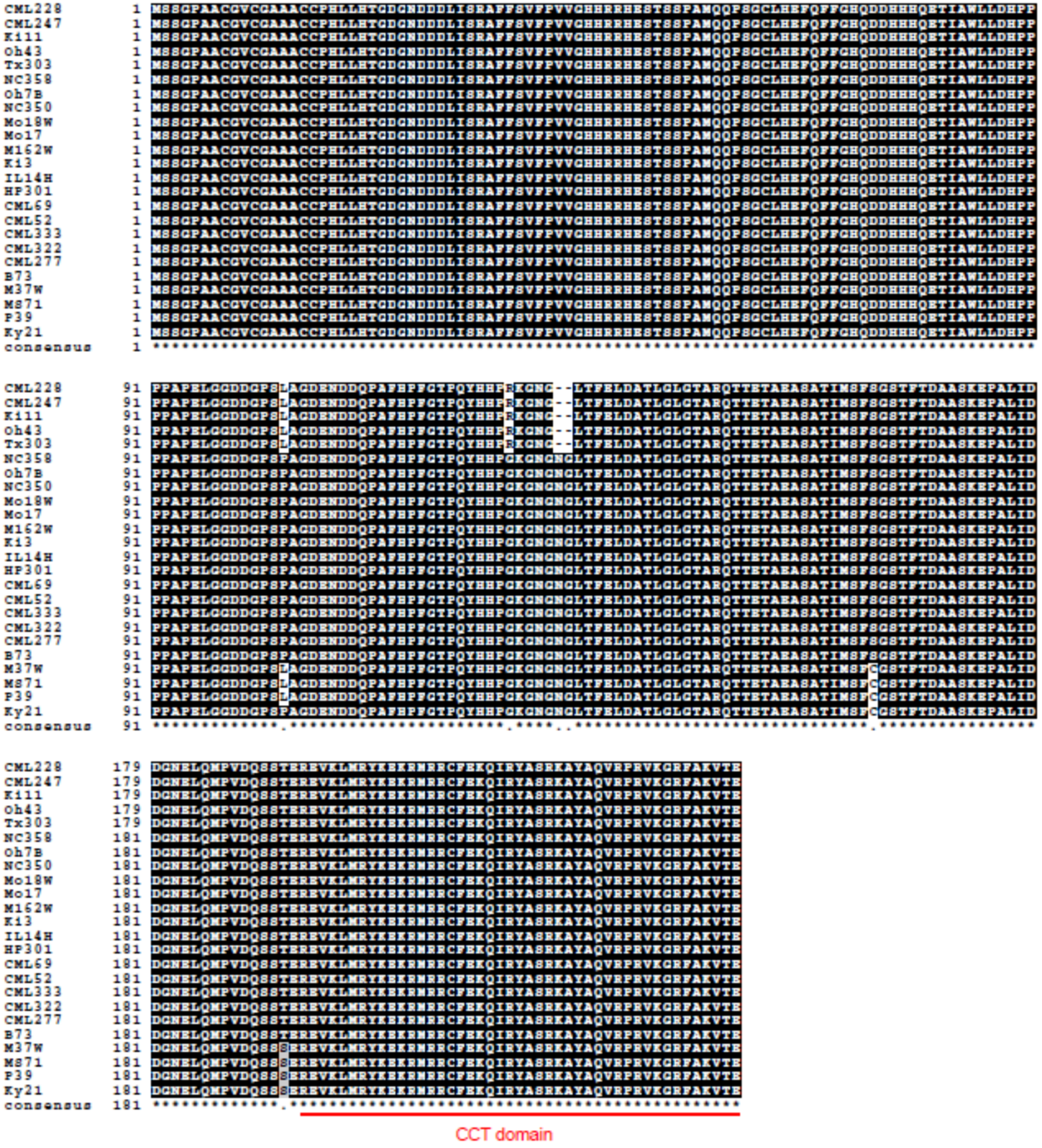
CML228
CML247
Ki11
Oh43
Tx303
NC358
Oh7B
NC350
Mo18W
Mo17
M162W
Ki3
IL14H
HP301
CML69
CML52
CML333
CML322
CML277
B73
M37W
MS71
P39
Ky21
consensus
CCT domain

Figure S9

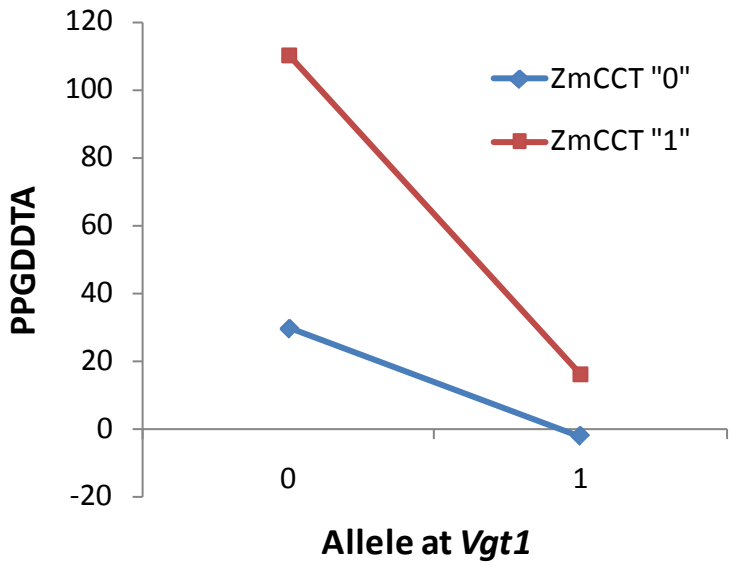
120
100
80
60
40
20
0
-20
PPGDDTA
0
1
Allele at *Vgt1*
ZmCCT "0"
ZmCCT "1"

Figure S10

Table S1. Comparison of QTL positions between days to silking under long daylengths (reported in Buckler 2009), photoperiod response silking QTLs, and growing degree days to silk under long daylengths re-analyzed here.

---

NAM Map marker numbers (m1 – m1106) indicating peak position of long day silk QTL and support intervals of photoperiod response silk QTL:

| chrom | photoperiod left SI | long day QTL peak | photoperiod right SI | cM distance |
|---|---|---|---|---|
| 1 | m66 | m67 | m69 | 0 |
| 1 | m107 | m115 | m119 | 0 |
| 1 | m144 | m154 | m156 | 0 |
| 2 | m200 | m201 | m203 | 0 |
| 2 | m284 | m284 | m286 | 0 |
| 3 | m324 | m319 | m331 | -1.5 |
| 3 | m410 | m411 | m412 | 0 |
| 4 | m487 | m489 | m488 | 5.5 |
| 6 | m690 | m706 | m702 | 14.7 |
| 7 | m805 | m810 | m814 | 0 |
| 8 | m902 | m903 | m904 | 0 |
| 9 | m972 | m972 | m977 | 0 |
| 9 | m992 | m998 | m994 | 4.9 |
| 10 | m1062 | m1062 | m1067 | 0 |

NAM Map marker numbers indicating peak position of long day silk QTL from original analysis (days to silk, Buckler et al, 2009) and reanalysis (growing degree days, current paper).

| days to silk | GDD to silk |
|---|---|
| m27 | m9 |
| m45 | m41 |
| m67 | m67 |
| m90 | m115 |
| m116 | m154 |
| m150 | m201 |
| m201 | m232 |
| m219 | m284 |
| m232 | m314 |
| m265 | m319 |
| m285 | m367 |
| m314 | m406 |
| m325 | m411 |
| m368 | m445 |
| m400 | m489 |

m411
m445
m489
m510
m549
m596
m625
m659
m676
m685
m706
m746
m758
m771
m798
m816
m837
m845
m895
m927
m970
m998
m1063
m1103

m523
m549
m626
m676
m706
m746
m767
m810
m903
m926
m972
m998
m1062
m1102

Table S2. Variance components for family (pop) main effect and marker within family selected from final joint linkage models for photoperiod responses in growing degree days to silk and anthesis and also for days to silk under long daylengths (from Buckler et al., 2009).

| Factor | Variance component | Proportion of total variance |
|---|---|---|
| *Silk GDD photoperiod response* | | |
| pop | 91.14 | 0.11 |
| m69*pop | 36.42 | 0.04 |
| m114*pop | 9.23 | 0.01 |
| m156*pop | 9.22 | 0.01 |
| m201*pop | 7.73 | 0.01 |
| m285*pop | 13.29 | 0.02 |
| m325*pop | 10.44 | 0.01 |
| m412*pop | 13.41 | 0.02 |
| m488*pop | 10.64 | 0.01 |
| m693*pop | 7.45 | 0.01 |
| m810*pop | 4.75 | 0.01 |
| m903*pop | 18.44 | 0.02 |
| m974*pop | 67.79 | 0.08 |
| m993*pop | 38.64 | 0.05 |
| m1063*pop | 76.70 | 0.09 |
| Residual | 439.20 | 0.51 |
| Total | 854.50 | |
| Mean QTL variance | | 0.03 |
| *Anthesis GDD photoperiod response* | | |
| pop | 94.28 | 0.12 |
| m5*pop | 4.61 | 0.01 |
| m69*pop | 22.62 | 0.03 |
| m110*pop | 6.34 | 0.01 |
| m157*pop | 6.01 | 0.01 |
| m285*pop | 13.88 | 0.02 |
| m356*pop | 12.57 | 0.02 |
| m410*pop | 14.85 | 0.02 |
| m487*pop | 9.28 | 0.01 |
| m683*pop | 5.95 | 0.01 |
| m903*pop | 25.42 | 0.03 |
| m973*pop | 71.99 | 0.09 |
| m993*pop | 32.61 | 0.04 |
| m1063*pop | 56.22 | 0.07 |
| Residual | 386.09 | 0.51 |
| Total | 762.71 | |
| Mean QTL variance | | 0.03 |
| *Days to silk (long daylengths)* | | |
| pop | 2.02 | 0.27 |

| | | |
|---|---|---|
| m27*pop | 0.06 | 0.01 |
| m45*pop | 0.08 | 0.01 |
| m67*pop | 0.21 | 0.03 |
| m90*pop | 0.04 | 0.01 |
| m116*pop | 0.07 | 0.01 |
| m150*pop | 0.07 | 0.01 |
| m201*pop | 0.07 | 0.01 |
| m219*pop | 0.05 | 0.01 |
| m232*pop | 0.10 | 0.01 |
| m265*pop | 0.06 | 0.01 |
| m285*pop | 0.18 | 0.02 |
| m314*pop | 0.05 | 0.01 |
| m325*pop | 0.15 | 0.02 |
| m368*pop | 0.08 | 0.01 |
| m400*pop | 0.13 | 0.02 |
| m411*pop | 0.14 | 0.02 |
| m445*pop | 0.07 | 0.01 |
| m489*pop | 0.06 | 0.01 |
| m510*pop | 0.03 | 0.00 |
| m549*pop | 0.05 | 0.01 |
| m596*pop | 0.04 | 0.00 |
| m625*pop | 0.04 | 0.01 |
| m659*pop | 0.04 | 0.01 |
| m676*pop | 0.04 | 0.01 |
| m685*pop | 0.03 | 0.00 |
| m706*pop | 0.05 | 0.01 |
| m746*pop | 0.08 | 0.01 |
| m758*pop | 0.04 | 0.00 |
| m771*pop | 0.06 | 0.01 |
| m798*pop | 0.03 | 0.00 |
| m816*pop | 0.10 | 0.01 |
| m837*pop | 0.03 | 0.00 |
| m845*pop | 0.03 | 0.00 |
| m895*pop | 0.20 | 0.03 |
| m927*pop | 0.07 | 0.01 |
| m970*pop | 0.07 | 0.01 |
| m998*pop | 0.31 | 0.04 |
| m1063*pop | 0.31 | 0.04 |
| m1103*pop | 0.06 | 0.01 |
| Residual | 2.22 | 0.29 |
| Total | 7.60 | |
| Mean QTL variance | | 0.01 |

Table S3. Variance components for genotype main effects (Vg), genotype by daylength interaction (Vg*d), and their ratio (Vg*d/Vg) for GDDTA from the analysis of all NAM RILs (overall) and analysis of subsets of NAM RILs derived from crosses between B73 and tropical or non-Stiff Stalk (NSS) temperate founders only. Environments were grouped into long daylength ($n$ = 8) or short daylength ($n$ = 3) environments. All genotype by environment interaction variance components were significant ($p$ <0.0001) based on likelihood ratio tests.

| | Overall | Tropical | NSS |
|---|---|---|---|
| Vg | 1174.87 | 544.02 | 909.28 |
| Vg*d | 211.19 | 189.92 | 38.34 |
| Vg*d/Vg | 0.18 | 0.35 | 0.04 |

Table S4. Primers used to sequence six regions around and including *ZmCCT* gene on chromosome 10 in 27 NAM founders and 16 teosinte (*Zea mays* subsp. *parviglumis*) inbred lines.

| Region | Forward primer | Reverse primer |
|---|---|---|
| A1 | ATGTAGGCCCATTCAGCATATC | TATTGCAGTTGGCAATTGAGAC |
| A2 | TTATTTTAGGACAGAGGCATGGA | TTATCTGCTTCTCAAAGCACCTC |
| A3 | TCATAGCATCAGGCATCAGC | TACATCAGTGGGCGTACCAA |
| A4 | TATCTGCTCCTTCCTCCATCTC | TGCACCAGAGTGTCTTTTGTCT |
| A5 | AGGAGACACCCCTAGCCAAT | AGCTTGGGAGGGAGATTTGT |
| A6 | CACTTATCCTCGCTCGATCTCT | GGACGTGTTGAGTACCAATGAA |

*ZmCCT* gene regions sequenced in 16 teosinte inbred lines

| | | | | *ZmCCT* regions sequenced | | | | | |
|---|---|---|---|---|---|---|---|---|---|
| Name | Race | Accession | Location | A1 | A2 | A3 | A4 | A5 | A6 |
| TIL01 | Balsas | Ames 28399 | Tzitzio, Michoacan | | | X | X | X | |
| TIL02 | Balsas | na | Ixcapuzalco, Guerrero | | X | X | | | |
| TIL03 | Jalisco | Ames 28400 | La Lima, Jalisco | X | | X | X | X | X |
| TIL04 | Balsas | na | Teloloapan, Guerrero | X | | X | X | X | X |
| TIL05 | Balsas | na | S. Pedro Juchatengo, Oaxaca | X | X | X | X | X | |
| TIL06 | Balsas | Ames 28401 | Palo Blanco, Guerrero | X | X | | X | X | |
| TIL07 | Balsas | Ames 28402 | Tierra Colorada, Guerrero | X | | X | X | X | |
| TIL08 | Balsas | na | Tepoztlan, Morelos | X | X | X | X | X | |
| TIL09 | Balsas | Ames 28403 | Tejupilco, Mexico | X | | X | X | X | |
| TIL10 | Balsas | Ames 28404 | Teloloapan, Guerrero | X | X | | X | X | |
| TIL11 | Jalisco | Ames 28405 | Amatlan de Cañas, Nayarit | X | X | | X | X | X |
| TIL12 | Jalisco | na | Huitzuco, Guerrero | X | | X | X | X | X |
| TIL14 | Jalisco | Ames 28406 | El Rodeo, Jalisco | X | | X | X | X | |
| TIL15 | Balsas | Ames 28407 | Palo Blanco, Guerrero | X | X | | X | X | X |
| TIL16 | Balsas | Ames 28408 | Palo Blanco, Guerrero | X | | X | X | X | X |
| TIL17 | Balsas | Ames 28409 | Teloloapan, Guerrero | X | | X | | | X |

Table S5. Sequence variation at six regions including or adjacent to *ZmCCT* on chromosome 10 within the NAM founders or teosinte inbreds.

| region | maize | | | | | teosinte | | | | | $\pi_{maize}/\pi_{teosinte}$ | $\theta_{maize}/\theta_{teosinte}$ |
|---|---|---|---|---|---|---|---|---|---|---|---|---|
| | N | L | S | π | θ | N | L | S | π | θ | % | % |
| A1 | 25 | 611 | 24 | 0.010 | 0.010 | 14 | 596 | 37 | 0.020 | 0.020 | 50.2 | 52.3 |
| A2 | 25 | 579 | 16 | 0.010 | 0.007 | 7 | 569 | 23 | 0.013 | 0.017 | 73.3 | 43.1 |
| A3 | 27 | 687 | 24 | 0.008 | 0.009 | 12 | 638 | 30 | 0.012 | 0.016 | 67.3 | 58.2 |
| A4 | 27 | 698 | 12 | 0.003 | 0.004 | 12 | 690 | 20 | 0.010 | 0.010 | 29.2 | 46.5 |
| A5 | 27 | 719 | 46 | 0.020 | 0.017 | 14 | 698 | 60 | 0.030 | 0.030 | 66.7 | 56.7 |
| A6 | 27 | 703 | 43 | 0.010 | 0.016 | 7 | 749 | 57 | 0.031 | 0.031 | 30.9 | 51.2 |

*N*, number of sequence; *L*, the length of a given region; *S*, number of segregating sites

Table S6. Sequence diversity in A6 region upstream of *ZmCCT* transcription start size within maize diversity panel lines carrying B73 alleles at SNP1411 and SNP1520 or carrying alternate alleles.

| Allele | *N* | *L* | *S* | π | θ |
|---|---|---|---|---|---|
| B73 allele | 207 | 566 | 5 | 4E-04 | 0.002 |
| NonB73 allele | 23 | 618 | 45 | 0.032 | 0.02 |

*N*, number of lines; *L*, sequence length; *S*, number of segregating sites

Table S7. Primers used on maize - teosinte crosses for fine mapping, allelic effects estimation, and allele specific expression assays.

| Marker Name | Type | AGP v2 position | Experiment | Gene | Forward Primer | Reverse Primer |
|---|---|---|---|---|---|---|
| PZD00121.indel | indel | 89373055 | FM | GRMZM2G097605 | GCAAGAGGTGGCATGCTTAT | TGGATGCAACTATGCTGGAA |
| PZD00122.1 | SNP | 90285522 | FM | GRMZM2G072632 | TTGATTGAAGTCGGTCACCA | GAACTTGAGGAAGGCGACTG |
| PZD00123.1 | SNP | 90492009 | FM | GRMZM2G166694 | CAATTGGCCCACCTACTTGT | ATGGAAGGCCTCACCAGAG |
| PZD00124.1 | SNP | 90815727 | FM | GRMZM2G089163 | CTGTATTGGGTCCCCTGAGA | TATGTCTCTGCGCTCGATTG |
| PZD00125.indel | indel | 90933576 | FM | GRMZM5G807276 | CCAAATGGGGTCCAATAAAA | CACGTACGCTCAATCGTGAA |
| PZD00126.indel | indel | 91170803 | FM | GRMZM2G039381 | ACCAGCACCTGGACTAATGG | CAAGCCACTCGAACTGACAA |
| PZD00127.indel | indel | 91858067 | FM | GRMZM2G419826 | AGGAGTCCAGCAATCAGTGG | GCGGCATGGATCATTAGATTA |
| PZD00128.1 | SNP | 92135358 | FM | GRMZM2G176998 | GCAGTTAGAGTCCGCAGGAG | TCCACGTTCATCACGAAGAT |
| PZD00129.1 | SNP | 92831244 | FM | GRMZM2G025939 | GCACCTATCATCACTGCTCCT | CCATGTTAAAGCCGGAACTC |
| PZD00130.1 | SNP | 94103269 | FM | GRMZM2G174671 | TCTTCTCCTGGCAACGATTT | TCTGGGAACAGGGATTGTTT |
| PZD00131.1 | SNP | 94249426 | FM | ZmGHD7-exon1 | CTATCCCGAAGGATTGTCCA | GTCGTCTGCTGTGGTGGAG |
| PZD00131.indel | indel | 94251114 | AE, ASE | ZmGHD7-Exon 1 | FAM-TCATCACCGTCGTCATGAGT | CGCTTGCTTCTGCTGTCTC |
| PZD00132.indel | indel | 94251314 | FM | ZmGHD7-exon2 | CCTCCCAAGCTAGTCGATCC | TGTGCGTAAAGTGCAACTCA |
| PZD00133.indel | indel | 94251565 | FM | inter genic space | GGACGAGACTCCATCTCTGG | AAGGCAGGTTGCGCTTATAG |
| PZD00134.indel | indel | 94590294 | FM | GRMZM2G077951 | CAGACCATCCGTTCTCAACA | GAGCGTGCGGAGAGAATAAG |
| PZD00135.indel | indel | 94700222 | FM | GRMZM2G176737 | TGTCCGTGAACCTTGATTGA | GCGGTGGTTGTAGTAGAGGAA |
| PZD00136.1 | SNP | 98706403 | FM | GRMZM2G007721 | TCAATGGCAGAACTCACAGC | TGCCACGCAAATTCTACAAG |
| PZD00137.1 | SNP | 100227596 | FM | GRMZM2G017164 | CATACCGATGAGCCATGTTG | GGGCTCGAATATTCCACTGA |
| PZD00138.1 | SNP | 101006267 | FM | GRMZM2G004211 | TGGGTTTATCAGACAGGGACA | CATCTTCATCCTGCGACAAA |
| PZD00139.1 | SNP | 105923266 | FM | GRMZM2G471186 | GACTCTGGACGCATCCTTTC | GAGTCAGCGACAGCATCAAA |
| PZD00140.1 | SNP | 107901476 | FM | GRMZM2G090441 | CGTCCGTAGCGTCCTACCTA | ATTACGCCGGTGCATATTG |
| PZD00141.1 | SNP | 108377411 | FM | GRMZM2G059965 | GCATCATGCAGATCCGTAAC | GCGTCTCCGTATCCAGTGAT |
| PZD00142.1 | SNP | 108854876 | FM | GRMZM2G085892 | CCAGTATATCGCGCCTGTCT | ACCAGTCCACCAGGAACC |
| PZD00143.1 | SNP | 109803542 | FM | GRMZM2G151041 | AATGGCTTGCCAATTTACCA | AGAACCTCATTCGCCACAAG |
| PZD00144 | GBS | 94451428 | FM | upstream of ZmGHD7 | CTGCTGTTTGGCAACAAATTGTGGGCCGGACAGCAGACTCCACAACAGTGATGGCG GCTGTTAC[1] | |
| PZD00145.indel | indel | 94249426 | FM | ZmGHD7-intron | TGGACAATCCTTCGGGATAG | TGAGTTGCACTTTACGCACA |
| PZD00146.indel | indel | | AE | ZmGHD7 upstream | CTCTGGCAGGATTGGAAAAT | CTACCGGAGAATGGGGTTTC |

[1]GBS sequence read

Table S8. Origins of the teosinte parents used in crosses for the allelic effect estimation and allele specific expression assays.

| Name | Subspecies | Race | Collector | Accession | Location |
|---|---|---|---|---|---|
| *A. Teosinte parents for the allelic effect estimation* | | | | | |
| TIL01 | parviglumis | Balsas | JSGyLOS | Ames 28399 | Tzitzio, Michoacan |
| TIL03 | parviglumis | Jalisco | JSGyMAS | Ames 28400 | La Lima, Jalisco |
| TIL11 | parviglumis | Jalisco | JSGyMAS | Ames 28405 | Amatlan de Cañas, Nayarit |
| TIL14 | parviglumis | Jalisco | Benz | Ames 28406 | El Rodeo, Jalisco |
| TIL16 | parviglumis | Balsas | Beadle & Kato | Ames 28408 | Palo Blanco, Guerrero |
| TIL25 | mexicana | Central Plateau | Puga | | Degollado, Jalisco |
| Parent2007 | parviglumis | Balsas | Beadle & Kato | CIMMYT 8778 | Valle de Bravo, Mexico |
| Parent2009 | parviglumis | Balsas | Beadle & Kato | CIMMYT 8759 | Teloloapan, Guerrero |
| *B. Teosinte parents for the allele specific expression assay crosses* | | | | | |
| TIL01 | parviglumis | Balsas | JSGyLOS | Ames 28399 | Tzitzio, Michoacan |
| TIL03 | parviglumis | Jalisco | JSGyMAS | Ames 28400 | La Lima, Jalisco |
| TIL05 | parviglumis | Balsas | JSG | | S. Pedro Juchatengo, Oaxaca |
| TIL09 | parviglumis | Balsas | JSGyLOS | Ames 28403 | Tejupilco, Mexico |
| TIL11 | parviglumis | Jalisco | JSGyMAS | Ames 28405 | Amatlan De Cañas, Nayarit |
| TIL14 | parviglumis | Jalisco | Benz | Ames 28406 | El Rodeo, Jalisco |
| TIL16 | parviglumis | Balsas | Beadle & Kato | Ames 28408 | Palo Blanco, Guerrero |
| TIL25 | mexicana | Central Plateau | Puga | | Degollado, Jalisco |

Table S9. $F_1$ crosses between inbred lines of temperate maize and teosinte used in allele specific expression assays.

| Maize Parent | Teosinte Parent (see Table S8) | Number of Biological Replicates |
|---|---|---|
| OH43 | TIL01 | 5 |
| OH43 | TIL03 | 4 |
| B73 | TIL05 | 3 |
| OH43 | TIL09 | 4 |
| OH43 | TIL10 | 5 |
| B73 | TIL11 | 4 |
| W22 | TIL11 | 5 |
| OH43 | TIL15 | 4 |
| B73 | TIL25 | 5 |
| W22 | TIL25 | 4 |

Table S10: Amplicon sizes of parent alleles at *ZmCCT* amplified for gene expression analyses.

| Maize Parent | Allele Size |
|---|---|
| B73 | 340/341 |
| CML103 | 334/335 |
| Ki3 | 340/341 |
| Mo17 | 340/341 |
| OH43 | 334/335 |
| W22 | 340/341 |

| Teosinte Parent | Allele Size |
|---|---|
| TIL1 | 340/341 |
| TIL3 | 340/341 |
| TIL5 | 334/335 |
| TIL9 | 340/341 |
| TIL10 | 343/344 |
| TIL11 | 334/335 |
| TIL14 | 340/341 |
| TIL15 | 346/347 |
| TIL25 | 334/335 |